Digital capacitive angular-position sensor

E.B. Mohammed and M. Rehman

Abstract: A capacitive angular position sensor capable of covering 360° is presented. It is made up of four quadrants, each of which consists of a parallel plate capacitor whose higher potential plate (HPP) has a specific shape. A grounded semi-circular plate, whose angular position is measured, moves between these capacitors. When these capacitors are supplied with sinusoidal voltages of mutually shifted phases in a bridge system, the phase of the output voltage of the bridge changes with the mechanical angle. Simulation results show that this relationship can be linearised if the shape of the HPPs is modified. A simple proto-type has been developed in which the shaping of the HPPs gives satisfactory improved results. The phase of the output voltage is measured digitally and the relationship between the angular position and the digital output is found to be linear, with a linearity error $\pm 0.5\%$ and a resolution of 3 arc minutes.

1 Introduction

Since capacitive position sensors are becoming increasingly popular, many methods [1–3], have been introduced to deal with the conversion of the capacitance changes into displacements. Some of these, for instance [1] and [2] using a modified Martin oscillator with a micro-controller or a switched capacitor interface, are unable to handle capacitance changes at frequencies higher than 10 Hz [4]. Another method [3] based on virtual rotor grounding is unable to cover the full 360° range. Compared to inductive displacement sensors, the developed sensor geometries are typically planar structures which make it smaller in size and this size can be easily varied. Also the frequency range for inductive sensors is generally much smaller than that of capacitive sensors. Inductive sensors, unlike encoders, do not contain brushes and are therefore not united by the problems associated with brushes such as wear-and-tear and friction. Inductive sensors can also, unlike optical/sensors, operate in dusty environments.

In our technique, we have taken a grounded semi-circular rotor that moves between the plates of four quadrant capacitors. This rotor shields part of the active area of the capacitor plates during its angular movement. The extent of this shielding depends on the rotor position. The mechanical arrangement used permits coverage of the full-circle range (360°) i.e. angular displacement for one complete mechanical revolution of the rotor. When the arrangement is connected to an electronic circuit, we obtain a linear relationship between the mechanical angle and the digital output, which can be interfaced with a personal computer or micro-controller to control the angle. All these features of the sensor are novel.

2 Theory

The sensor mainly consists of three circular conducting, coaxial parallel plates of the same radii. These plates are:

(a) higher potential plate (HPP): as shown in Fig. 1*a* this is a fixed circular disc that contains three annular rings; the inner and outer rings are grounded to serve as guards. The middle ring contains four capacitors, (C_1,..., C_4), each covering 90° that are insulated from one another. These segments are supplied with sinusoidal signals that have the same amplitude. However, the signals of each pair of adjacent segments have a phase difference of 90° [5]. These segments are supplied with the appropriate signals through a grounded shield wire as shown in Fig. 2.

(b) lower potential plate (LPP): as can be seen in Fig. 1*b* this plate is similar to the (HPP) except that its middle circle is not segmented. This middle plate acts as a common plate for the four segments of the (HPP) with them it develops four capacitances (C_1, C_2, C_3, and C_4). A thin shielded wire is attached to the common plate of the (LPP) to pass the currents (i_1, i_2, i_3 and i_4) that are produced when the segments are supplied with their specified signals (see Fig. 2).

(c) Shielding plate: as shown in Fig. 1*c*. this is a semi-circular, grounded plate that is fixed on a shaft which passes through the centres of all the three plates. The grounded plate is kept between the LPP and the HPP. During rotation, it covers an active area equal to half the total area of the segments at any instant, thereby varying the values of the capacitors and modifying the currents passing into the LPP. The position of the shielding plate thus decides the currents to be summed up and the output voltage V_o, since the later is the product of the summed currents and a pure resistance R (see Fig. 2).

Each of the capacitors ($C_1 \ldots . C_4$) has a capacitance that is determined by the effective overlap area between the shielding plate and the LPP. This can be described through the well-known capacitance equation:

$$C = \varepsilon . A/d \tag{1}$$

where ε is the permittivity, A is the effective plate area and d is the distance between the HPP and LPP.

Since A, in this case, is the area of a sector, it can be expressed by:

$$A = (r_1^2 - r_2^2)\theta/2 \tag{2}$$

IEE Proceedings online no. 20030002

doi:10.1049/ip-smt:20030002

Paper first received 17th January 2002 and in revised form 29th July 2002

The authors are with the Department of Electronics Engineering, Z.H. College of Engineering and Technology, A.M.U., Aligarh-202002 (U.P.), India

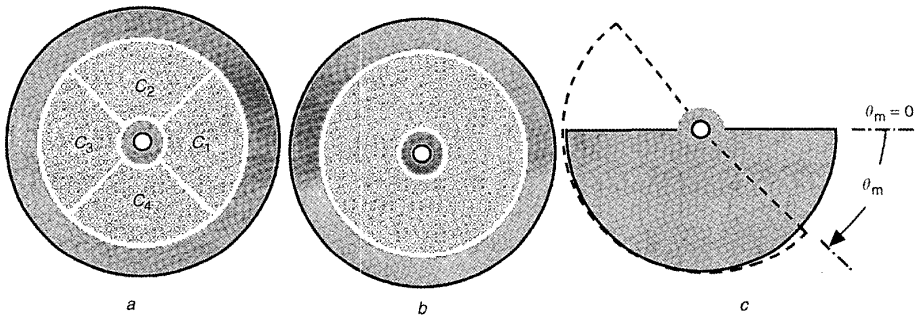

Fig. 1
a HPP
b LPP
c Semi-circular shielding plate (θ_m is the mechanical angle of movement)

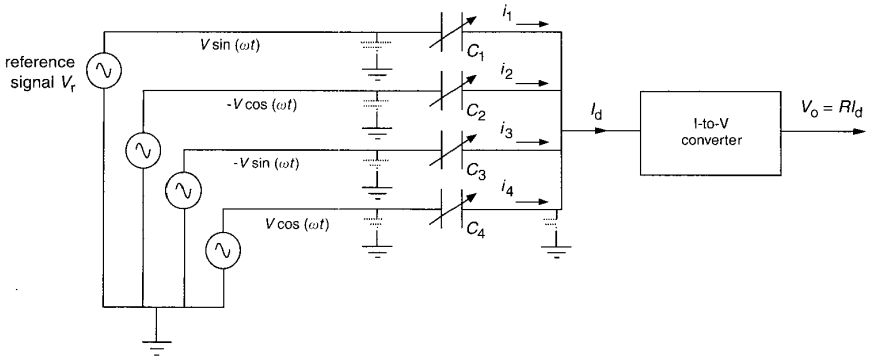

Fig. 2 *Electrical representation that relates the plate's capacitances to their signals and the reference and output signals*

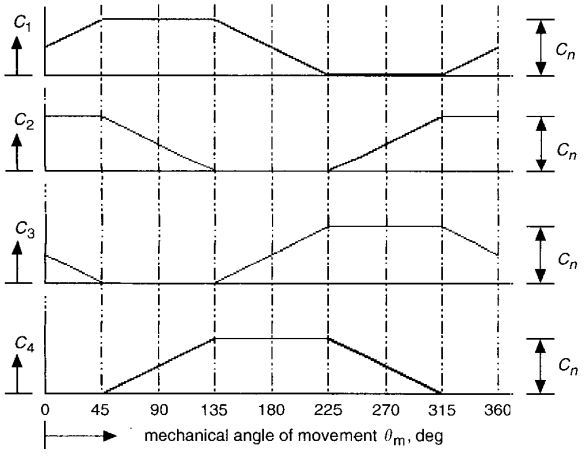

Fig. 3 *The capacitance variations during one complete revolution of the rotor*

where r_1 and r_2 are the radii of the outer and inner circles and θ is the central mechanical angle (in radians) covered by the segment. Therefore, any change in the angular position of the shielding plate will change the effective area of some sectors and consequently the value of their capacitances. Fig. 3 shows the variation of these capacitances as a function of the mechanical angle of the movement.

These changes in the capacitances causes the phase of the output signal to change, since these capacitances are electrically connected. The grounded semi-circular moving plate shields an area equal to half of the total area of the plates, but at least one segment from the HPP will have its effective area unaltered for movement over a range of 90°. This depends on the position of the moving plate. Because the moving plate is used as a shield, its alignment, tilt, etc will not affect the operation of the system, because its slightly tilted position will not affect the shielding process.

Any vibrations of the moving plate in the axial direction will not affect the effective capacitance whilst radial vibrations may have a temporary affect on the effective capacitance. Stray capacitances will either appear across the supply or across the detector and hence become ineffective. Both the shield and the guard electrodes were properly implemented inorder to keep fringing effects well defined as well as low, and the system free from grounding noise and pick-up. The electrical phase of the output voltage in the circuit of Fig. 2 changes over 360° when the moving plate completes one full mechanical revolution. The output voltage V_o can be given by:

$$V_o = RL_d = R\sum_{i=1}^{4} I_i = RV\omega\{(C_2 - C_4)\sin\omega t + (C_1 - C_3)\cos\omega t\} = K_1\{(C_2 - C_4)\sin\omega t + (C_1 - C_3)\cos\omega t\} \quad (3)$$

$$= K_1K_2\sin(\omega t + \phi) \quad (4)$$

where $K_1 = RV\omega$, $K_2 = \{(C_2 - C_4)^2 + (C_1 - C_3)^2\}^{1/2}$ and $\phi = \arctan\{\{(C_1 - C_3)/(C_2 - C_4)\}$.

Because of the alternate changes in these capacitances (from maximum to minimum and *vice versa*), the above argument changes over a range of 90° for each quarter of the complete cycle. This argument carries the complete output phase information. Let the capacitance of the segment that is fully overlapped with the LPP be denoted by C_n (see Fig. 3). The electrical and mechanical phases with respect to the reference supply signal and reference mechanical angle are ϕ_n, θ_n respectively, and then the argument of the output signal ϕ_p can be given by:

$$\phi_p = \phi + \phi_n + 90 \tag{5}$$

where $\phi = \arctan\{(C_{n-1} - C_{n+1})/C_n\}$, $n = 1 \ldots 4$ over a complete circle and C_0 is taken as C_4 and C_5 is taken as C_1. Equation (5) is more clearly represented in Table 1. The symmetry between the electrical and mechanical systems means that the mechanical angle θ_m can be given by:

$$\theta_m = \theta + \theta_n + 90 \tag{6}$$

Table 1: Plate in full overlap with the LPP and the corresponding phase angle

Plate in full overlap	Electrical angle ϕ, deg	Range of ϕ, deg
C_1	$90+\tan^{-1}\{(C_4-C_2)/C_n\}$	45–135
C_4	$180+\tan^{-1}\{(C_3-C_1)/C_n\}$	135–225
C_3	$270+\tan^{-1}\{(C_2-C_4)/C_n\}$	225–315
C_2	$360+\tan^{-1}\{(C_1-C_3)/C_n\}$	315–45

This sensor works on the principle of comparing the phase of the output signal V_o with the phase of the reference signal V_r.

3 The Sensor Prototype Design including shaping the HPP for linear output

With the arrangements discussed in the preceding Sections, signal is found to be completely dependent on the tangent formula, which is a well-known non-linear quantity. In order to minimise this non-linearity, the shape of each segment of the HPP is modified. To compensate for the condition that the tangent gives a higher value than required (as in the range from 0–45° of Fig. 4), the radii difference r of C_{n-1} (which is C_1 in this case) will be decreased by a factor f (i.e. r becomes $r(1-f)$, or f is a per-unit decrease of radii difference) and that of C_{n+1} increased by the same factor to become $r(1+f)$. At the same time the radius of the LPPs middle circle was increased to $r(1+f)$. This factor f, takes the value $f=0$ (when $\phi = 0°,45°,90° \ldots$.) since the repetition of the tangent at these extreme values lies on a linear straight line. Based on the fact that the design factor takes the value of zero every 45°, the basic equation for this design factor f can be written as

$$f = k(\phi - N)(N + 45 - \phi) \tag{7}$$

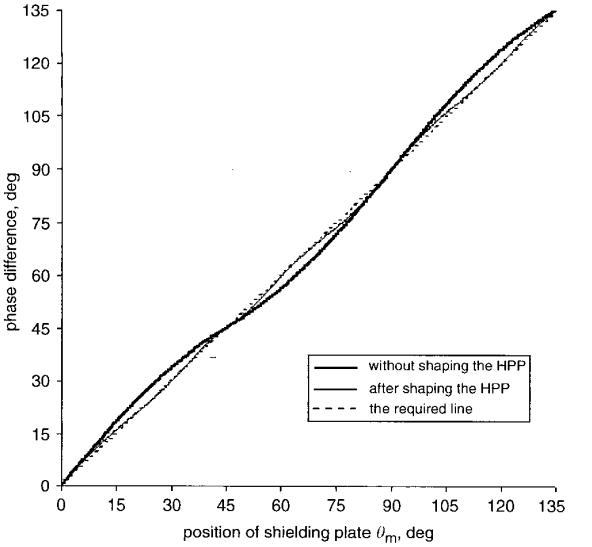

Fig. 4 *The output signal*

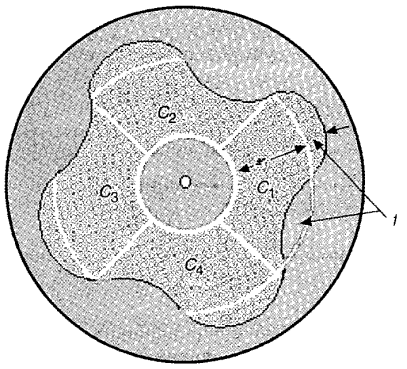

Fig. 5 *The new shape of the HPP*

$N = 0°,45°,90°,135°.....315°$ and $0° \leq (\phi - N) \leq 45$, k is a weighting factor. The choice of k is based on a purely empirical format. The practical significance of the above equation is to produce concave and convex ends for each of the HPP segments as shown in Fig. 5. These modifications are made such that they are cyclic for all the plates. It is found practically that this reduces the dependency on the tangent formula. This can be seen clearly in the simulation results of Fig. 4, in which the best value for the weighting factor is chosen to be $k = 0.0009$. This value for k gives a design factor of $0 \leq f < 0.46$ which is practically accepted, since f is the per unit increase or decrease of the radii difference r.

4 Experimental Set-up and Results

Fig. 6 shows the detailed signal processing circuit diagram of the experimental set-up with which the angular displacement sensor compares the phase of the output with the phase of the reference-input signal of the electronic circuit and generates counts that are proportional to the phase difference between the two signals. Both the start and stop control signals for the counter are taken as ramp pulses sampled from the reference and the output, respectively, and they are at the rate of single ramp pulse per cycle. At the start the signals coincide with each other. Moving the shielding plate, the position of the ramp sampled from the output changes, and the counter measures the phase between the two signals. Although the circuit has a single analog input signal of 10 kHz, 20 V_{pp} sinusoidal-wave, its output is in digital form, hence it is a digital angular position sensor. The input against the output transfer characteristic curve of the sensor is shown in Fig. 7. As

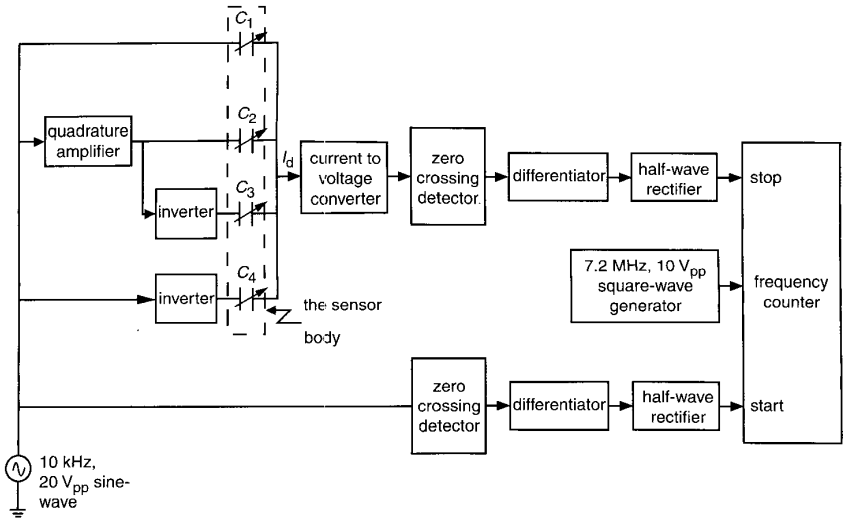

Fig. 6 *The detailed circuit diagram of the capcitive angular position sensor*

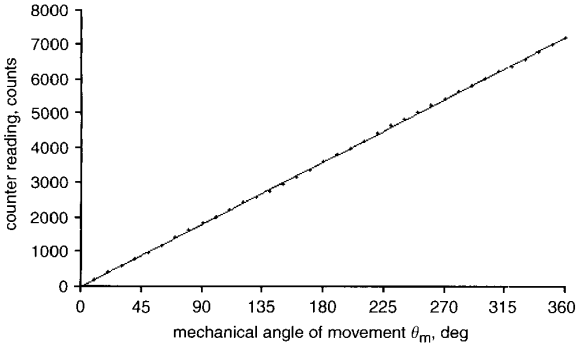

Fig. 7 *Counter readings against the angular position after shaping the electrodes*

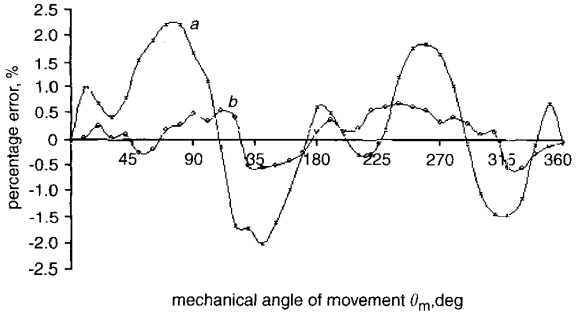

Fig. 8 *The measurement errors*
a Before shaping the electrodes
b After shaping the electrodes

shown here the plot is linear over the full 360° range and has a conversion gain of 20 counts per degree [6]. For comparison and to give a clearer image, the percentage linearity errors before and after shaping of the electrodes are plotted in Fig. (8). For the prototype model, only a small error exists, plot *b*, the curve shows that this error is predominantly random in nature, which will definitely be improved with improvements in the fabrication techniques. In addition, absolutely linear results are not reached by the designed factor (see Fig. 4). The mp can be employed to further linearise the performance.

5 Conclusions

In this paper, a sensitive digital angular position sensor has been presented which can, for instance, be used with industrial robots; for throttle flap positioning or steering in vehicles. The system is implemented with simple electrodes and inexpensive electronic components. When this circuitry is accurately fabricated it can be used to replace expensive angular position systems. By shielding the wires and guarding the electrodes, the sensor capacitance was found to vary from zero to 3 PF which is sufficient for the intended application.

6 Acknowledgments

The authors wish to acknowledge the University Grants Commission–India for their support of this work in the form of JRS for Eisa.

7 References

1 LI, X., MEIJER, G.C.M., DE JONG, G.W., and SPRONCK, J.W.: 'An Accurate Low-cost Capacitive Absolute Angular-Position Sensor With a Full-Circle Range', *IEEE Trans. Instrum. Meas.*, 1996, **45**, (2), pp. 516–519
2 TOTH, F.N., and MEIJER, G.C.M.: 'A Low-cost, Smart Capacitive Position Sensor', *IEEE Trans. Instrum. Meas.*, 1992, **41**, (6), pp. 1041–1044
3 BRASSEUR, G., FULMEK, P.L., and SMENTANA, W.: 'Virtual Rotor Grounding of Capacitive Angular Position Sensor', *IEEE Trans. Instrum. Meas.*, 2000, **49**, (5), pp. 1108–1111
4 LOTTERS, J.C., OLTHUIS, W., VELTINK, P.H., and BERGVELD, P.: 'A Sensitive Differential Capacitive to Voltage Converter for Sensor Applications', *IEEE Trans. Instrum. Meas.*, 1999, **48**, (1), pp. 89–96
5 WOLFFENBUTTEL, R.F., and FOERSTER, J.A.: 'Non-contact Capacitive Torque Sensor For Use on Rotating Axle', *IEEE Trans. Instrum. Meas.*, 1990, **39**, (6), pp. 1008–1013
6 GAYAKWAD, R.A.: 'Op-Amps and Linear Integrated Circuits', 10, (Prentice-Hall of India New Delhi, 3rd edn), pp. 430–438.